ECCOMAS Congress 2016
VII European Congress on Computational Methods in Applied Sciences and Engineering
M. Papadrakakis, V. Papadopoulos, G. Stefanou, V. Plevris (eds.)
Crete Island, Greece, 5–10 June 2016

DEVELOPMENT OF A CENTRIFUGAL BLOOD PUMP FOR ECMO AND VAD OPERATIONS

Shinhwa Choi[1], Nahmkeon Hur[1*], Mohammad Moshfeghi[2], Seongwon Kang[1], Wonjung Kim[1]

[1]Department of Mechanical Engineering, Sogang University
Seoul,04107 Korea
[*]e-mail: nhur@sogang.ac.kr

[2] Multi-Phenomena CFD ERC, Sogang University
Seoul,04107 Korea
e-mail: mmoshfeghi@sogang.ac.kr

Keywords: Centrifugal blood pump, Extra corporeal membrane oxygenation (ECMO), CFD

Abstract. *Using cardiopulmonary circulatory assist devices has been increased in the recent years as more models are available in the market. These devices can be employed in the situation during which both cardiac and respiratory support to a patient's heart and lungs have to be provided, either during or after surgeries, for short time or even in the case of severe disease, for a period of weeks. Hence, it is critical to know the details of the phenomena happen inside a blood pump from both mechanical performances (such as pressure head and mechanical efficiency) and biomedical factors (such as hemolysis and thrombosis) and to design an optimum pump from both aspects. This paper investigates development of centrifugal blood pump impeller, specifically with focusing on the performances during ECMO condition. The baseline model is designed by investigating existing commercial pumps and considering results of recirculation, pressure heads and mechanical efficiencies together with their biomechanical performance via Modified Indices of Hemolysis (MIH). Afterword, two more modified models are designed and simulated. Overall, a comprehensive comparison between the results of all three case demonstrate that when impeller radius and prime volume is smaller, recirculation is reduced at impeller and MIH value becomes lower. Additionally, high scalar shear stress is observed near the volute and impeller walls and inside the top cavity gap.*

1 INTRODUCTION

As number of patients with cardiovascular disorders has increased, using cardiopulmonary circulatory assist devices has been increased as well. These devices can be used when heart and lungs cannot perform their normal duties, such as surgeries and diseases. Cardiopulmonary circulatory assist devices are divided into two types. First, ventricular assist device (VAD) which are devices for patients of heart failure. And second, extra corporeal membrane oxygenation (ECMO) is devices for patients of cardiovascular and respiratory diseases. VAD is composed of blood pump and driving parts. Pressure drop is comparatively low in blood pump in VAD. On the other hand, an ECMO system is composed of a blood pump, a driving devices and oxygenator. ECMO has higher pressure drop because of its multi-component design [1]. In previous study investigated existing pump to find out effect of impeller diameter and rotational speed on performance of pump running in turbine model [2]. Koki et al. [3] investigated hemolysis inside centrifugal blood pump through flow visualization. Yuki et al. [4] and Yukihiko et al. [5] established the design process of centrifugal blood pump. In order to figure out hemolytic phenomenon inside of centrifugal blood pump, mathematical models are adopted with CFD simulation. The mathematical models are divided into two types [6,7]. First, Eulerian approaches consider all areas contributing to the hemolysis [6]. Second, Lagrangian approaches miss out several high scalar shear stress areas. So Lagrangian approaches can't accurately measure [7]. In this research a baseline model via designed by investigating the existing commercial blood pumps [8], by considering the results of CFD simulations, performance curves and bio-mechanical factor analyses such as hemolysis. Furthermore, the baseline model is modified according to its hemolysis performance in ECMO condition, and two more geometries are designed and simulated. The results are presented and compared in terms of flow characteristic, pump performance curve and the hemolysis index of pumps.

2 PHYSICS AND GOVERNING EQUATIONS

In present paper, incompressible steady flow is assumed. Therefore, the governing equations can be present as:

$$\nabla \cdot \mathbf{u} = 0 \tag{1}$$

$$\frac{\partial \mathbf{u}}{\partial t} + \mathbf{u} \cdot \nabla \mathbf{u} = -\nabla \left(\frac{P}{\rho} \right) + \nu \nabla \cdot \nabla \mathbf{u} \tag{2}$$

where $\mathbf{u}$ is the velocity vector, P is the pressure and ν is kinetic viscosity.

The blood pumps rotational speed is 1200~3600 rpm which is associated with Re≈ 1.2×10^5 (based on the impeller diameter). Hence, current study has to be conducted using turbulent assumptions. Therefore, the standard k-ε turbulence model has been adopted. The standard k-ε turbulence model can be present as:

$$\frac{\partial (\rho k)}{\partial t} + div(\rho k \mathbf{U}) = div\left[\frac{\mu_t}{\sigma_k} grad(k) \right] + \mu_t E_{ij} \cdot E_{ij} - \rho \varepsilon \tag{3}$$

$$\frac{\partial (\rho \varepsilon)}{\partial t} + div(\rho \varepsilon \mathbf{U}) = div\left[\frac{\mu_t}{\sigma_\varepsilon} grad(\varepsilon) \right] + C_{1\varepsilon} \frac{\varepsilon}{k} 2\mu_t E_{ij} \cdot E_{ij} - C_{2\varepsilon} \rho \frac{\varepsilon^2}{k} \tag{4}$$

Where $C_\mu = 0.09$, $\sigma_k = 1.00$, $\sigma_\varepsilon = 1.30$, $C_{1\varepsilon} = 1.44$ and $C_{2\varepsilon} = 1.92$ is constant.

The rotational motion of the impeller has been simulated by sliding grid method. In order to consider the non-Newtonian properties of blood, the Carreau model has been applied for blood viscosity simulation [9]. The adopted Carreau model reads as:

$$\mu = \mu_\infty + (\mu_0 - \mu_\infty)(1 + (\lambda\dot{\gamma})^2)^{(n-1)/2} \tag{5}$$

Where λ=3.313 s, n=0.3568, μ_0=0.056 Pa-s and μ_∞=0.00345 Pa-s are constants used for the non -Newtonian viscosity of blood.

3 MIH CALCULATION

Hemolysis is related to exposure of red blood cells to high shear stresses, which destroys of red blood cells [10,11]. In order to evaluate hemolysis index, ASTM F1841-97 standard [12] suggests three methods for blood damage evaluations caused by high shear stresses of a medical device: normalized index of hemolysis (NIH), normalized milligram index of hemolysis (mgNIH), modified index of hemolysis (MIH). In current study, the MIH is adopted. The numerical calculations are based on work of Wurzinger et al. [13] and Giersiepen et al. [14] who propose a power law-based model for a damage index as:

$$D = C\tau^{\alpha} t^{\beta} \tag{6}$$

where $C = 3.62\times10^{-7}$, $\alpha = 2.416$, $\beta = 0.785$ are constants defined by analysis of the experimental data, τ is shear stress and t is the time of exposure.

Moreover, Bludszuweit [15] suggests a shear stress parameter using the scalar shear stress derived from six components of the stress tensor. The scalar shear stress can be presented as:

$$\tau_{vm} = \left[\frac{1}{2}\left[\left(\sigma_{xx}-\sigma_{yy}\right)^2 + \left(\sigma_{yy}-\sigma_{zz}\right)^2 + \left(\sigma_{zz}-\sigma_{xx}\right)^2 + 6\left(\sigma_{xy}^2+\sigma_{yz}^2+\sigma_{zx}^2\right)^2\right]\right]^{\frac{1}{2}} \tag{7}$$

In order to evaluate MIH, Garon and Farinas [7] suggest numerical model, which calculates blood damage through volume integration of a damage factor. The linear damage function can be present as:

$$\bar{D}_l = D^{1/0.785} = \left(3.62\times10^{-7}\right)^{1/0.785} \tau^{2.416/0.785} t \tag{8}$$

$$D(\tau,t) = \left(\bar{D}_l\right)^{0.785} \tag{9}$$

and finally the MIH can be present as:

$$MIH = D(\tau,t)\times10^6 \tag{10}$$

According to comparison presented by Chang et al. [16], the MIH values calculated based on this method in agreement with experiment.

4 GEOMETRY OF PUMPS

The geometry pumps is determined based on work done by Chang et al [16] and their investigation on the existing commercial blood pumps. Later, two more modified models are also designed and simulated. The 3-D geometries are shown in Figure 1. All pumps have blade-type impeller with a shroud. To design the blade, β_2 is chosen as certain value and β_1 is calculated, according to velocity triangle as shown in Figure 2.

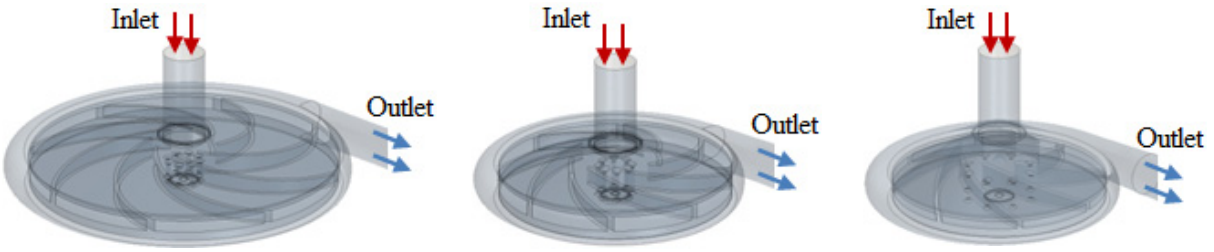

(a) Prototype 1 (baseline) (b) Prototype 2 (c) Prototype 3

Figure 1: Isometric view of the degined models.

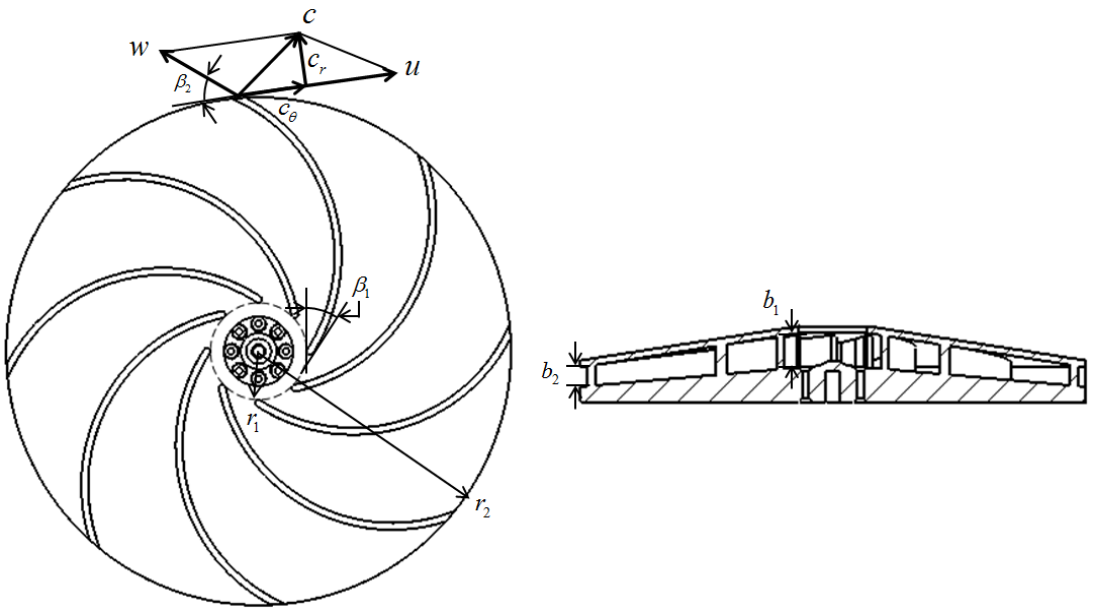

Figure 2: Convention for blade profile and velocity triangle.

$$\beta_1 = \text{atan}\left(c_{m_1} / w_{\theta_1}\right) \tag{11}$$

where $c_{m_1} = Q_{impeller\ inlet} / A_{impeller\ inlet}$. Later, the local β angle along to blade radius is calculated based number of blades and the impeller passage height at inlet and outlet.

The outlet pipe is connected to the casing by a volute designed based on Constant Momentum Volute (CMV) method [17]. The volume of the blood pumps, the radius of impeller and height of impeller inlet, outlet are listed in Table 1. The baseline model pump has the largest volume and longest radius of impeller. The third Prototype pump has the smallest volume and shortest impeller radius.

5 RESULTS AND DISCUSSIONS

The unsteady simulations are performed using STARCCM+ (v.9.06) at ECMO and VAD conditions. However, since the ECMO condition is more critical than the VAD, in the present research the flow properties of ECMO condition are presented. Convergence of each simulation is checked by pressure and velocity values at certain point in flow flied and residuals of mass and momentum conservation.

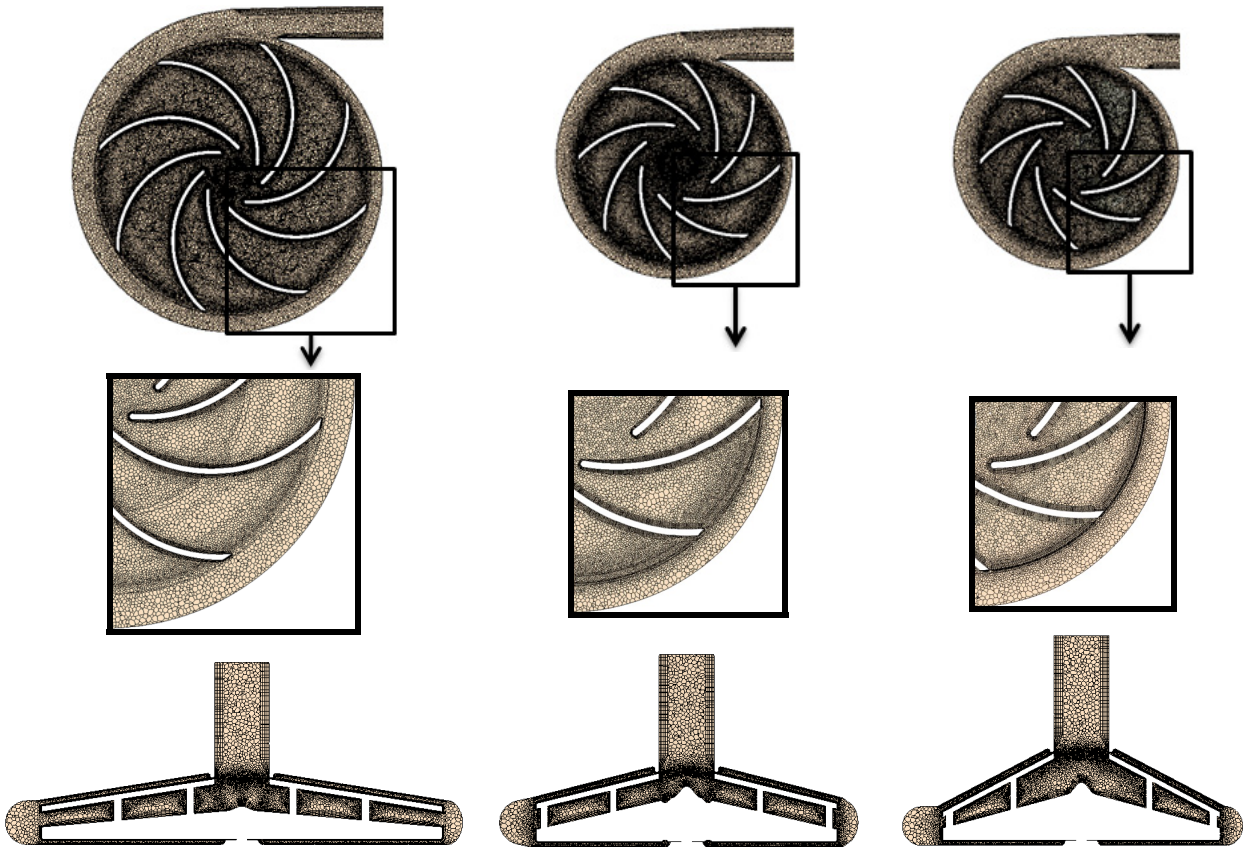

(a) Prototype 1 (baseline) (b) Prototype 2 (c) Prototype 3

Figure 3: Mesh arrangement of the designed models

	Volume [mL]	Radius of Impeller [mm]	β_1 [degree]	β_2 [degree]
Prototype 1	95	37	33	30
Prototype 2	75	27	16	40
Prototype 3	66	25	14	43

Table 1: Dimensions of the designed models.

In order to investigate the flow pattern inside the pumps, Figure 4 shows the changes in the pressure head (ΔP) with respect to the flow rate (Q). The performance curve is conducted by steady simulation to figure out the trends. In general, the pressure differences decrease with increasing flow rate. All cases have same trend, the largest difference is approximately 5000 [Pa] among the various flow rate. In centrifugal pump, difference of area between impeller inlet and outlet is a significant design parameter. Generally, head is controlled by difference of impeller inlet and outlet areas. The greater the difference between the areas of the impeller inlet and outlet the lower the pressure difference at the same rotational speed. For the same reason, Prototype 3 has the lowest pressure difference. So in present study Prototype 3 has the fastest rotational speed at ECMO condition to reach pressure required for ECMO condition, as shown Table 2.

Figure 5 shows velocity magnitude and streamlines for each Prototype at ECMO condition. The result of top section presents occurrence of recirculation at impeller exit area at right side of impeller and inside volute. This asymmetric recirculation is caused by non-uniform pres-

sure distribution in the volute. The side views show that effect of wash-out holes at the bottom and the wash-out cavity at top and bridge of top cavity. The washout hole diameter is 1 mm and top cavity bridge gap clearance is 0.2 mm. The top cavity flow has very fast velocity because of the narrow gap. This flow causes a noticeable swirl at impeller inlet area.

Figure 6 demonstrates pressure distribution at ECMO condition. The pressure reference point is located at pump inlet. The top view section presents non-uniform pressure distribution in the volute, and the area near the outlet pipe has the highest pressure. Especially, Prototype 3 has small pressure drop along the volute and its pressure distribution is more uniform. The side views show that effect of top cavity flow. Since the flow through top cavity has very fast velocity. The area near the impeller inlet has the lowest pressure.

Figure 7 shows the scalar shear stress distribution at ECMO condition, which is an important factor in analysis of hemolysis by Equations (8-10). The high scalar shear stresses area are located inside volute and outside of impeller walls. The side view plot shows the effect of top cavity flow, which causes the swirl flow and high scalar shear stress at the top cavity wall. The highest scalar shear stress is located in this narrow gap.

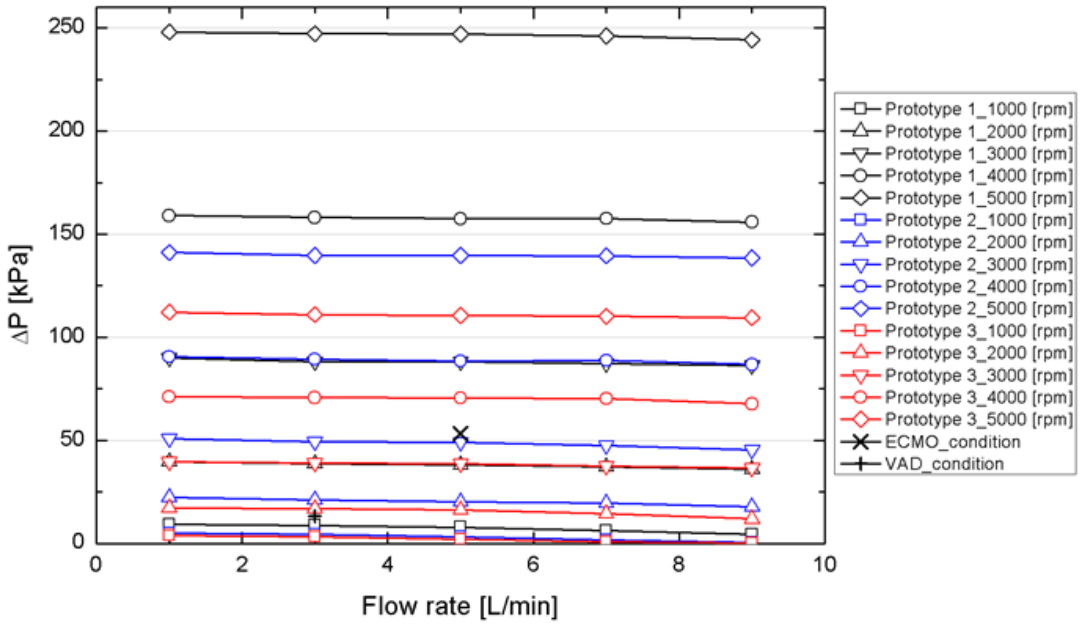

Figure 4: Pump characteristic curve

	Pressure difference [kPa]		Flow rate [L/min]		Rotational speed [rpm]	
	ECMO	VAD	ECMO	VAD	ECMO	VAD
Prototype 1 (baseline)	53	13	5	3	2368	1220
Prototype 2	53	13	5	3	3120	1670
Prototype 3	53	13	5	3	3619	1850

Table 2: ECMO and VAD operating condition

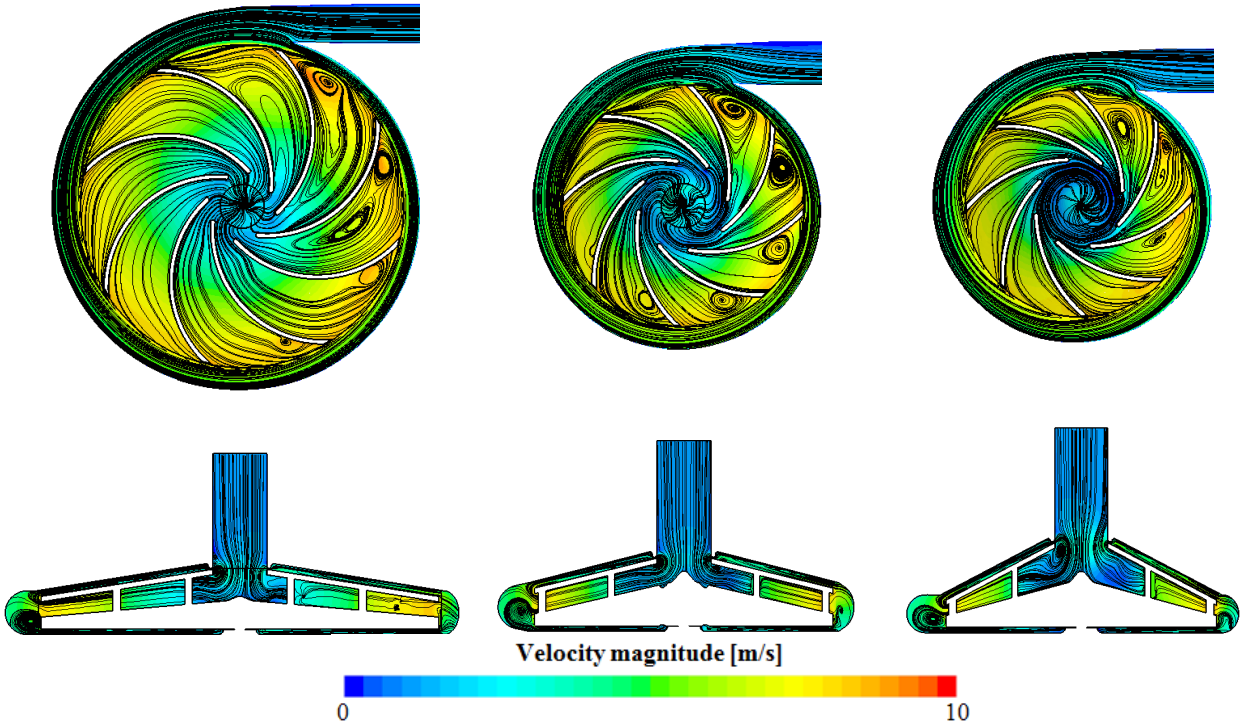

(a) Prototype 1 (baseline) (b) Prototype 2 (c) Prototype 3

Figure 5: Velocity magnitude and streamlines for designed pumps

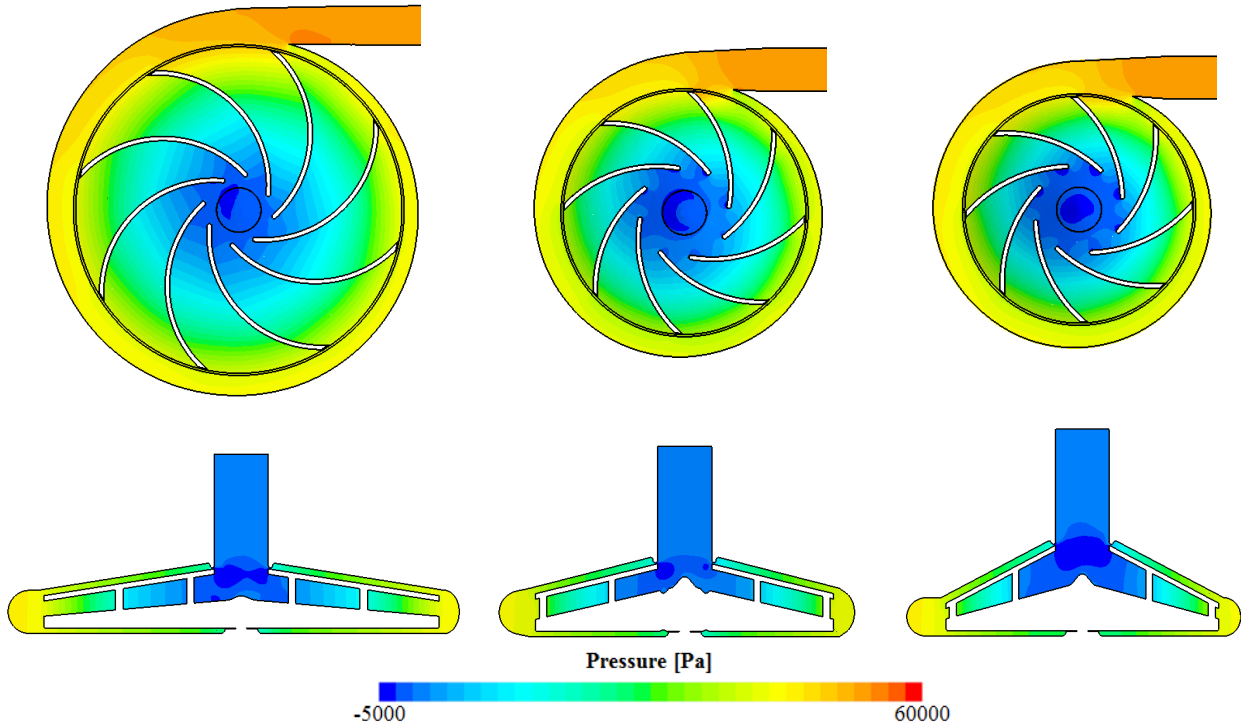

(a) Prototype 1 (baseline) (b) Prototype 2 (c) Prototype 3

Figure 6: Pressure distribution for designed pumps

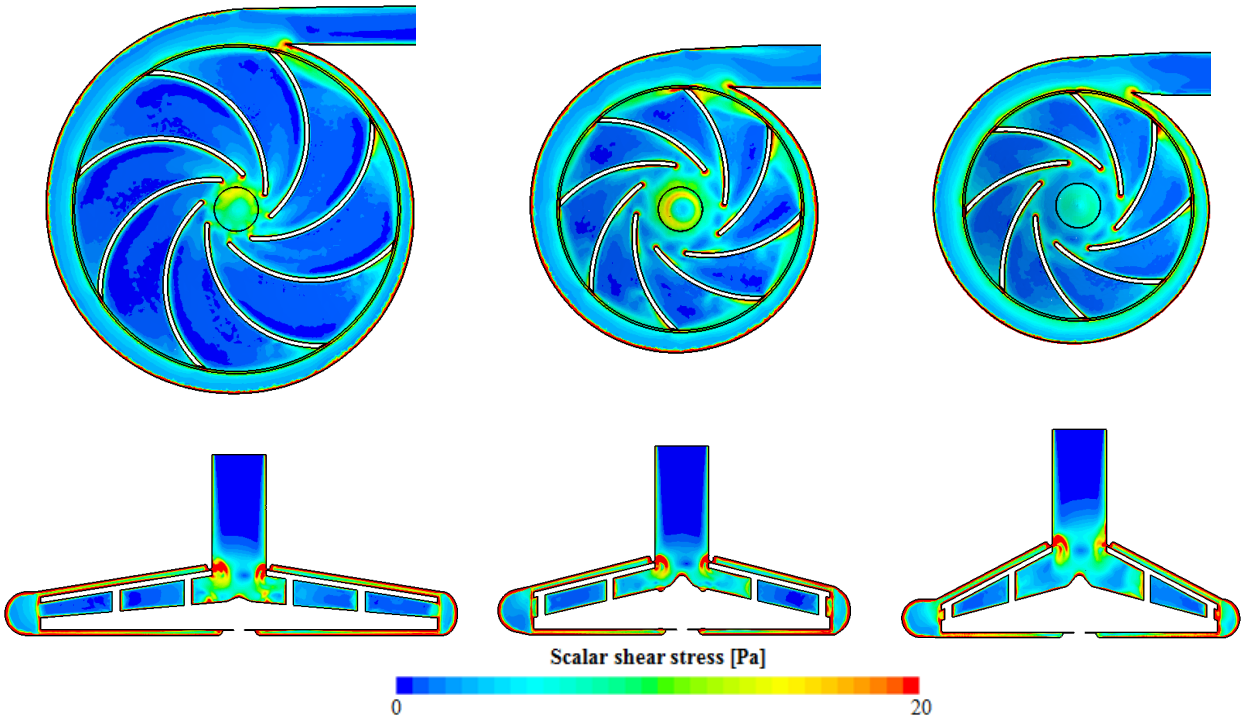

(a) Prototype 1 (baseline) (b) Prototype 2 (c) Prototype 3

Figure 7: Scalar shear stress distribution for designed pumps

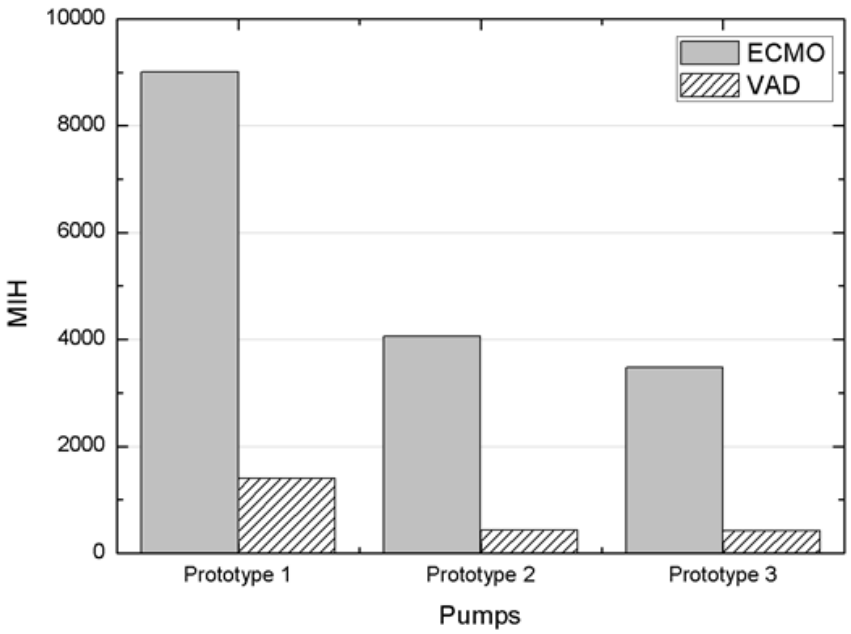

Figure 8: MIH values for designed pumps

Finally, Figure 8 displays the MIH value for three Prototypes at ECMO and VAD conditions. As it is seen, the VAD condition has smaller MIH value, because the rotational speed of the VAD condition is slower than the ECMO condition. In addition, a comparison between three models reveals that Prototype 3 has the fastest rotational speed while it has the lowest MIH values under ECMO and VAD conditions. Based on the result, the size of impeller and

priming volume are found to be more important variables than impeller rotational speed to occur hemolysis.

6 CONCLUDING REMARKS

In the present study, three different centrifugal blood pumps are designed and investigated through numerical simulation, using standard k-ε turbulence model and sliding grid technique. In order to draw performance curve and figure out mechanical performance trend steady simulations are conducted with various flow rate (1-9 [L/min]) and rotational speed (1000-5000 [rpm]). As a result, all models have same trend. The pressure difference is reduced with increasing flow rate. Hence Prototype 3 has the lowest pressure difference because Prototype 3 has the largest difference between impeller inlet and outlet area. The results of flow streamlines show that all prototype pumps have asymmetric recirculation at the impeller exit area. The gap flow through top cavity has fast velocity. So it causes the swirl flow at impeller inlet area. Corresponding to the velocity magnitude and streamlines result, pressure is non-uniform in the volute. Because of gap flow through top cavity, the area near the impeller inlet has the lowest pressure. The results of scalar shear stress distribution, which is an important factor in analysis of hemolysis, show that high scalar shear stresses are located in volute wall, top cavity wall and impeller outside wall. At narrow gap of top cavity the highest scalar shear stress is observed. From the bio-mechanical aspect, in order to calculate MIH, an Eulerian approach is used. As result reveal, Prototype 3 has the smallest MIH value despite higher rotational speed than other models under ECMO and VAD conditions. According to results the size of impeller and total pump volume are important variables in generating the hemolysis.

ACKNOWLEDGMENTS

This research was supported by a grant of the Korea Health Technology R&D Project through the Korea Health Industry Development Institute (KHIDI), funded by the Ministry of Health & Welfare, Republic of Korea (grant number : HI14C0746).

REFERENCES

[1] J.F. Fraser, K. Shekar, S. Diab, K. Dunster, S.R. Foley, C.I. McDonald, M. Passmore, G. Simonova, J.A. Roberts, D.G. Platts, D.V. Mullany, Y.L. Fung, ECMO-the clinician's view. *International Society of Blood Transfusion (ISBT) Science Series*, **7**, 82-88, 2012.

[2] S.V. Jain, A. Swarnkar, K.H. Motwani, R.N. Patel, Effects of impeller diameter and rotational speed on performance of pump running in turbine model. *Energy Conversion and Management,* **89**, 808-824, 2015.

[3] K. Takiura, T. Masuzawa, S. Endo, Y. Wakisaka, E. Tatsumi, Y. Taenaka, H. Takano, T. Yamane, M. Nishida, B. Asztalos, Y. Konishi, Y. Miyazoe, K. Ito, Development of Desogn Methods of a Centrifugal Blood Pump with In Vitro Test, Flow Visualization, and Computational Fluod Dynamics: Results in Hemolysis Tests. *Artificial Organs,* **22**, 393-398, 1998.

[4] Y. Miyazoe, T. Sawairi, K. Ito, Y. Konishi, T. Yamane, M. Nishida, B. Asztalos, T. Masuzawa, T. Tsukiya, S. Endo, Y. Taenaka, Computational Fluid Dynamics Analysis

to Establish the Design Process of a Centrifugal Blood Pump: Second Report. *Artificial Organs,* **23**, 762-768, 1999.

[5] Y. Nose, Design and Development Strategy for the Rotary Blood Pump. *Artificial Organs*, **22**, 438-446, 1998.

[6] M.E. Taksin, K.H. Fraser, T. Zhang, C. Wu, B.P. Griffith, Z.J. Wu, Evaluation of Eulerian and Lagrangian Models for Hemolysis Estimation. *ASAIO Journal,* **58**, 363-372, 2012.

[7] A. Garon, M.I. Farinas, Fast Three-dimensional Numerical Hemolysis Approximation. *Artificial Organs,* **28**, 1016-1025, 2004.

[8] M. Chang, N. Hur, M. Moshfeghi, S. Kang, W. Kim, S.H. Kang, A Numerical study on Mechanical Performance and Hemolysis for Different Type of Centrifugal Blood pumps. *International Mechanical Engineering Congress & Exposition (IMECE),* Houston, Texas, USA, November 13-19, 2015.

[9] P.J. Carreau, Rheological Equations from Molecular Network Theories. *Journal of Rheology*, **16**, 99-127, 1972.

[10] L. Goubergrits, K. Affeld, Numerical Estimation of Blood Damage in Artificial Organs. *Artificial Organs*, **28**, 499-507, 2004.

[11] S.W. Day, J.C. McDaniel, PIV Measurements of Flow in a Centrifugal Blood Pump: Steady Flow. *Journal of Biomechanical Engineering*, **127**, 244-253, 2005.

[12] ASTM Committee, *Standard Practice for Assessment of Hemolysis in Continuous Flow Blood Pumps, Vol. ⅩⅢ,* Annual Book of ASTM Standard, F1841-97, 1997.

[13] L.J. Wurzinger, R. Opitz, H. Eckstein, Mechanical Bloodtrauma. An overview. *Angeiologie*, **38**, 81-97, 1986.

[14] M. Giersiepen, L.J. Wurzinger, R. Opitz, H. Reul, Estimation of Shear Stress-related Blood Damage in Heart Valve Prosteses-In Vitro Comparison of 25 Aortic Valve. *Artificial Organs*, **13**, 300-306, 1990.

[15] C. Bludszuweit, A Theoretical Approach to the Prediction of Haemolysis in Centrifugal Blood Pumps. *Ph.D. thesis,* University of Strathclyde Glasgow, Scotland, 1994.

[16] M. Chang, N. Hur, M. Moshfeghi, S. Kang, W. Kim, S.H. Kang, Investigation on Mechanical and Bio-mechanical Performance of a Centrifugal Blood Pump. *Journal of Computational Fluids Engineering*, **20**, 88-95, 2015.

[17] Karassik, J. Igor, *Pump hand book, 2th Edition*. McGraw Hill, 1986